Levelized electricity cost reduction of a 1 MWe multi-field solar thermal power plant

[1]Irfan Shaikh and [1]Anish Modi

[1]Department of Energy Science and Engineering, Indian Institute of Technology Bombay, Powai, Mumbai 400076, Maharashtra, India

Abstract

A levelized cost of electricity (LCOE) reduction opportunity for a 1 MWe multi-field solar thermal power plant in Jodhpur, India, without thermal storage has been identified and proposed. To generate useful heat, a multi-field solar thermal power plant utilizes two distinct concentrating solar fields—a parabolic trough collector and a linear Fresnel reflector. Feedwater from the power block in a parabolic trough solar thermal power plant is preheated using the cost-intensive parabolic trough collectors. A linear Fresnel reflector has been included for partial feedwater preheating to improve electricity generation economics. The linear Fresnel reflector solar collector field utilizes a saturated vapour at 250 °C and 40 bar pressure to preheat the incoming feedwater from 46.5 °C to 150 °C before entering the primary preheater. Techno-economic modelling and simulation were conducted using TRNSYS, and the levelized cost of electricity was reduced by 5% compared to the configuration without a feedwater heater.

Keywords: Linear Fresnel reflector, levelized cost of electricity, multi-field, parabolic trough collector

1. Introduction

Solar thermal power plant (STPP) technology has gained popularity worldwide for cleaner electricity generation. This is evident with a noted cumulative increase of six times the global STPP installations in the last decade (Feldman et al., 2021). The weighted average levelized cost of electricity (LCOE) has also come down by 68% over the past ten years, according to the International Renewable Energy Agency (IRENA, 2021). Globally, the most commercially implemented concentrating solar power (CSP) technology is the parabolic trough collector (PTC) that employs heat transfer fluid oil (Therminol VP-1) (Islam et al., 2018). Linear Fresnel reflector (LFR) is categorized as another line-focused CSP technology used to generate direct saturated steam.

Nomenclature

A_{ap}	aperture area of the collector (m^2)
C	cost of the system ($ or $ kWe or $ m^{-2})
CRF	capital recovery factor
d	discount rate
E	net electric energy (kWh)
h	enthalpy (J kg^{-1})
I	direct normal irradiance (W m^{-2})
LCOE	levelized cost of electricity ($ kWh^{-1})
$\dot{m}$	mass flow rate (kg s^{-1})
P	pressure (bar)
$\dot{Q}$	collector useful heat (W)
T	temperature (°C)
U	overall heat transfer coefficient (W m^{-2} K^{-1})

10.18086/swc.2023.03.11 Available at http://proceedings.ises.org

$\dot{W}$	Net electric power (W)
Greek symbols	
η	efficiency
Subscripts	
col	collector
d	design value
i	inlet
l	loss
m	mean
o	outlet
opt	optical

LFR collectors are considered economical in capital investment due to the ease of manufacturing slightly curved mirrors with ground installation and operation and maintenance costs due to simple stationary receivers and pipe joints (Hussain et al., 2017). However, the optical efficiency of the LFR collectors is less compared to PTC due to higher optical losses and tracking errors of the mirrors installed with reference to stationary receivers (Gunther, 2011). Intending to reduce the levelized cost of electricity (LCOE), several researchers have put forth innovative configurations and conducted a techno-economic analysis to compare a PTC and LFR-based STPP for electricity generation. Manzolini et al. (2011) conducted a steady-state design simulation of an STPP utilizing a novel configuration of a PTC solar field and molten salt as heat transfer fluid (HTF) to exploit direct and indirect steam generation. The innovation configuration resulted in a 6.5% cost decrease compared to the base scenario PTC STPP, indicating a potential path to lower LCOE.

Giostri et al. (2012) studied a performance comparison of different PTC STPP with different HTF (Therminol VP-1 and molten salt) with an innovative hybrid direct steam generation (DSG) and different HTF-based STPP. This study has reported that a hybrid DSG–-molten salt STPP increases solar-to-electricity conversion efficiency compared to alternative configurations due to its higher power block efficiency. A techno-economic comparison was conducted by Giostri et al. (2013) between PTC (indirect steam generation) and LFR (a combination of indirect and direct steam generation) configurations. This study concludes that the specific investment cost of the LFR technology must be halved compared to PTC to be cost-competitive. The leading cause is the decreased optical efficiency of the single-field LFR collectors utilized in the DSG process, which lowers the power plant's total efficiency. To realize the cost-benefit of a low-cost LFR collector compared to PTC, a multi-field STPP was proposed under the initiative of the Indian Institute of Technology Bombay and the Ministry of New and Renewable Energy (MNRE), India, in 2009. In the vicinity of New Delhi, India, a 1 MWe multi-field STPP comprising LFR and PTC solar fields and a superheated steam Rankine cycle-operated power block were commissioned and installed (Nayak et al., 2015). Desai and Bandyopadhyay (2015) conducted a techno-economic study featuring design optimization of a 1 MWe multi-field STPP without thermal energy storage for Jodhpur, India, to evaluate the cost-benefits of LCOE. Similar work on techno-economic modelling and analysis was carried out to reduce the LCOE using a solar tower with molten salt thermal energy storage along with a saturated and superheated LFR collector technology with phase change material (PCM) enhanced steam accumulator (Karandikar et al., 2021).

A 1 MWe multi-field (STPP) is made up of a low-cost and low-temperature LFR solar field to generate direct saturated steam, which is then combined with indirectly produced saturated steam before being superheated with a high-cost and high-temperature PTC solar field via Therminol VP - 1 HTF flowing through the steam generators. This combined saturated steam was heated to the turbine inlet temperature by the PTC solar field in the superheater. Earlier configuration from the literature (Desai and Bandyopadhyay, 2015) uses the heat produced by the PTC solar field for pre-heating the feedwater to a saturated water temperature of 250 °C from 46.5 °C before it enters the evaporator. This causes a substantial increase in the heat exchanger area and, therefore, the cost and a corresponding increase in the PTC solar field costs. As shown in Fig.1, a novel multi-field configuration has been proposed in this study to pre-heat the feedwater to 150 °C before it enters the preheater unit of the PTC solar field. Saturated steam at 250 °C would be the source of heat from a low-cost LFR solar field, which will condense to 150 °C using an open feedwater heater (OFWH) at the exit of the steam drum. This reduces the pre-heating heat load of the feedwater at the PTC side, eventually reducing the PTC solar field's collector area and the cost of net annual electricity production.

The present work is based on steady-state design point modelling and simulation of the novel configuration using Engineering Equation Solver (EES) (Klein and Nellis, 2021) and techno-economic modelling, simulation, and analysis using TRNSYS 18.0 (Klein et al., 2018). The results of the models reported in this research were compared to the published literature (Desai and Bandyopadhyay, 2015).

2. Design point modelling and simulation

2.1 Modelling methodology

Fig.1 shows the proposed configuration of the 1 MWe multi-field solar thermal power plant. The STPP is proposed to operate without fossil fuel and thermal energy storage backup. A Rankine cycle power block was used to generate electricity. The power cycle operates at an exit pressure of 0.1 bar and a turbine inlet design pressure of 40 bar. The turbine inlet temperature is set to 350 °C. A water-cooled steam condenser operating at a design pressure of 0.1 bar is employed. PTC and LFR solar fields are the source of heat input to the power block. PTC collector is designed to operate at the maximum operating temperature of 390 °C. The heat from the PTC solar field is transferred indirectly using Therminol VP-1 HTF (Eastman, 2019) oil to water/steam heat exchanger, whereas the heat from the LFR solar field is transferred through direct steam generation.

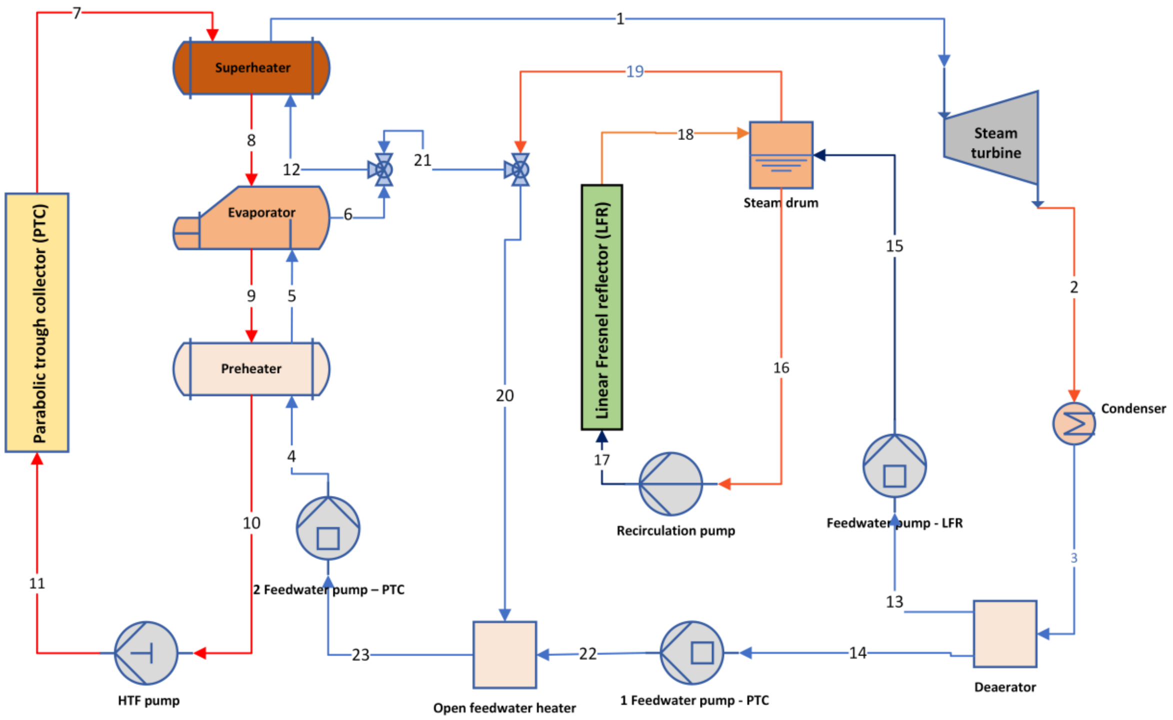

Fig. 1: Multi-field solar thermal power plant with open feedwater heater

During design operation, wet steam is produced with a designed exit vapour quality of 50 % in the LFR solar field receiver tubes. The wet steam is separated in a steam drum near the LFR receiver tube outlet and converted into saturated vapour and liquid. A recirculation pump is employed to return the saturated liquid to the LFR solar field receiver tube's inlet. The saturated vapour from the steam drum is fed to the control valve that allows the designed demanded source steam to the open feedwater heater implemented at the exit of the PTC feedwater pump for the pre-heating of PTC side feedwater. The exit condition of the feedwater heater is set at 150 °C before it is fed to the PTC preheater unit. Feedwater pumps pump the water to the desired operating pressure of 40 bar. The design parameters of the STPP are shown in Table 1. A steady-state design point modelling was carried out using the parameters in Table 1.

The steady-state characteristic equation of both the collector field has been used to evaluate the collector aperture area (Desai and Bandyopadhyay, 2015) given by

$$\eta_{\text{d,col}} = \eta_{\text{opt,col}} - \frac{U_{\text{l,col}} \cdot \Delta T_{\text{col}}}{I_{\text{d}}} \qquad \text{(eq. 1)}$$

where: $\eta_{\text{d,col}}$ = design solar field collector efficiency (%)

$\eta_{\text{opt,col}}$ = design solar collector optical efficiency (%)

$U_{\text{l,col}}$ = solar collector overall heat loss coefficient per unit aperture area, (W m^{-2} K^{-1})

$\Delta T_{\text{col}} = T_{\text{m,col}} - T_{\text{a}}$ = difference of solar collector mean and ambient temperature

$T_{\text{m,col}} = (T_{\text{o,col}} + T_{\text{i,col}})/2$ = mean temperature of the solar collector

I_{d} = design direct normal irradiance (W m^{-2})

Table 1: Design point parameters for a multi-field (PTC+LFR) 1 MWe STPP (Desai and Bandyopadhyay, 2015)

Design parameters	Value
Design direct normal irradiance	555 W m^{-2}
Optical efficiency of LFR	0.65
Optical efficiency of PTC	0.7
Overall heat loss coefficient for PTC and LFR	0.1 W m^{-2} K^{-1}
Isentropic efficiency of the turbine	65 %
Isentropic efficiency of the pumps	60 %
PTC collector outlet temperature	390 °C
Turbine inlet pressure	40 bar
Ambient temperature	30 °C
Heat exchanger pinch temperature difference	10 °C
Condenser pinch temperature difference	5 °C

$$\eta_{\text{d,col}} = \frac{\dot{Q}_{\text{d,col}}}{I_{\text{d}} \cdot A_{\text{ap,col}}} \qquad \text{(eq. 2)}$$

where: $\dot{Q}_{\text{d,col}}$ = collector useful thermal power produced by the collector receiver (MWt)

$A_{\text{ap,col}}$ = collector aperture area (m^2)

To estimate the unknown design parameters such as temperatures, mass flow rates, collector thermal capacities, heat exchanger duty and pump ratings, the energy and mass balance and respective characteristic equations of all the power plant components were solved in EES. The heat exchanger was modelled using the ε-NTU method to estimate the overall heat conductance of the heat exchanger (Patnode, 2006). A parametric study has been performed to evaluate the significance of adding an OFWH on the performance of the multi-field STPP. The following section discusses this parametric study.

2.2 Parametric study

It is intended to integrate OFWH at the exit of the LFR steam drum to preheat the feedwater from 46.5 °C to 150 °C before it enters the actual PTC preheater. The heat supplied to OFWH is through the saturated steam at 250 °C extracted from the LFR steam drum. It requires enlarging the collector aperture area of the LFR solar field to provide the OFWH with adequate heat for preheating the feedwater supplied to the PTC preheater. A parametric study was performed based on the collector aperture area of the PTC and LFR solar fields. An aperture area ratio (AR) has been defined as the ratio of the LFR collector area to that of the PTC aperture area. Fig. 2 shows the effect of increasing the (AR) on the thermal capacity of the power block. It shows that power block thermal capacity increases as the (AR) increases. This is because the power block's thermal capacity tends to rise when the thermal capacity of the OFWH increases. On the other hand, it diminishes as soon as the AR > 1, at which point the PTC thermal capacity has much reduced, lowering the OFWH capacity and the extraction mass flow rate that goes along with it for preheating.

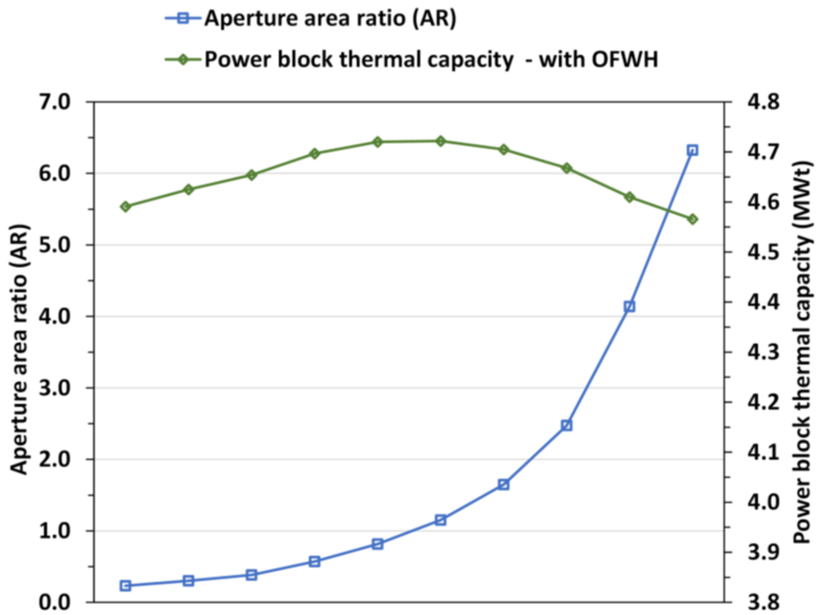

Fig. 2: Effect of increasing aperture area ratio on the power block thermal capacity

This trend has been illustrated in Fig. 3, which shows an increasing trend of the OFWH thermal capacity before AR<1 and a decreasing trend later. This is because when AR < 1, PTC's thermal capacity was more significant than the LFR's, necessitating higher extraction mass flow rates of saturated steam from the LFR solar field to the OFWH. The required extracted mass flow rate to OFWH decreased when LFR thermal capacity exceeded PTC thermal capacity at AR>1, and as a result, its thermal capacity gradually dropped as the LFR collector area increased. The PTC feedwater's design thermal capacity is declining, primarily because it is a function of PTC thermal capacity and falls as AR increases. Thus, the parametric study inferred that design point modelling and simulation must be carried out at the higher AR because it could benefit due to reduced heat exchanger and PTC collector area costs and improve the power generation's economy.

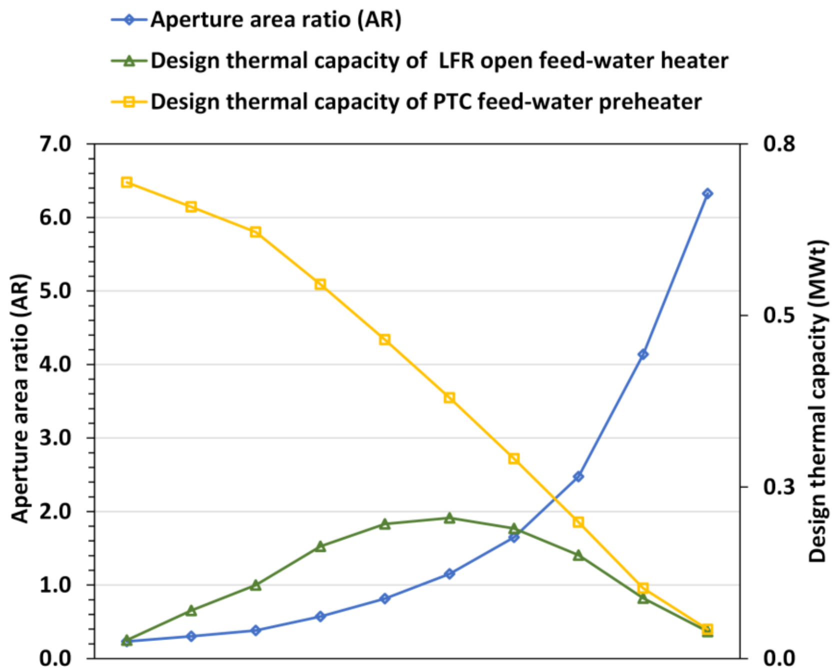

Fig. 3: Effect of increasing aperture area ratio on the OFWH and preheater thermal capacity

Table 2 lists the estimated design parameters of a novel 1 MWe multi-field STPP with open feedwater integrated at the outlet of the LFR steam drum.

Table 2: Calculated design parameters of the 1MWe multi-field STPP

Design parameters	Value
Collector aperture area of PTC	2617 m^2
Collector aperture area of LFR	10832 m^2
HTF mass flow rate through PTC solar field	2.72 kg s^{-1}
Feedwater mass flow rate to PTC – HX	0.22 kg s^{-1}
Feedwater mass flow rate to LFR – steam drum	1.37 kg s^{-1}
Saturated water mass flow rate through LFR	4.28 kg s^{-1}
Saturated steam mass flow rate to open feedwater heater	0.033 kg s^{-1}
PTC thermal rating	0.94 MWt
LFR thermal rating	3.66 MWt
Condenser thermal rating	3.51 MWt
PTC Collector efficiency	64.8 %
LFR Collector efficiency	61.0 %
Power block efficiency	21.6 %
Turbine gross power	1.025 MWe
Overall heat conductance of superheater	8392 W K^{-1}
Overall heat conductance of evaporator	12354 W K^{-1}
Overall heat conductance of preheater	2750 W K^{-1}

The quasi-steady modelling and simulation using TRNSYS 18.0 were carried out using the computed design parameters in Table 2. An off-design simulation in TRNSYS of a multi-field STPP with OFWH was performed to assess annual net power production from the STPP in Jodhpur, India. The steady-state thermodynamic values of a 1 MWe multi-field STPP with OFWH are detailed in Table 3.

Table 3: Steady-state design point state points of a 1 MWe multi-field STPP

State points	P	T	h	s	$\dot{m}$
	[bar]	[°C]	[kJ kg^{-1}]	[kJ kg^{-1} K^{-1}]	[kg s^{-1}]
1	40.0	350.2	3092.0	6.58	1.57
2	0.1	46.0	2437.0	7.69	1.57
3	0.1	46.2	192.6	0.65	1.57
4	40.0	150.2	634.5	1.84	0.23
5	40.0	250.5	1087.0	2.80	0.23
6	40.0	250.5	2801.0	6.07	0.23
7	13.0	390.2	-	-	2.73
8	12.0	322.6	-	-	2.73
9	10.0	260.5	-	-	2.73
10	8.5	243.4	-	-	2.73
11	13.6	243.8	-	-	2.73
12	40.0	250.5	2801.0	6.07	1.57
13	0.1	46.0	192.6	0.65	1.37
14	0.1	46.0	192.6	0.65	0.19
15	40.0	46.9	199.3	0.66	1.37
16	40.0	250.5	1087.0	2.80	4.29
17	45.0	250.8	1088.0	2.80	4.29

18	40.0	250.5	1944.0	4.43	4.29
19	40.0	250.5	2801.0	6.07	1.37
20	40.0	250.5	2801.0	6.07	0.03
21	40.0	250.5	2801.0	6.07	1.34
22	40.0	46.9	199.3	0.66	0.19
23	40.0	150.2	634.5	1.84	0.23

3. Techno-economic modelling and simulation

Techno-economic modelling was carried out using a performance and economic model of various components of the STPP. The performance or off-design modelling of the solar field and power block components was carried out using TRNSYS 18.0 (TRANSSOLAR Energietechnik GmbH, 2017). The model considered the off-design states of the LFR and PTC solar fields by using an incidence angle modifier correction from Morin et al. (2012) and Schenk et al. (2014). A flow following constant pressure and throttle-governed steam turbine has been employed to model the off-design electric power generation. The change in steam mass flow rate and turbine inlet temperature affects the turbine's isentropic efficiency. This change in the isentropic efficiency of the steam turbine due to the change in steam mass rate generation has been considered using an isentropic efficiency equation from the literature (Shang, 2000). Heat exchanger units were modelled using the ε–NTU method using the solar thermal electric component (STEC) library model (Schwarzbözl et al. 2002). Open feedwater heater, condenser, and pump units have been modelled using the thermal energy systems specialist (TESS) library (Thornton et al. 2012). The weather file used for the solar resource input data of direct normal irradiance and ambient temperature with 1-hour time resolution has been used for Jodhpur, India (Ramaswamy et al. 2013).

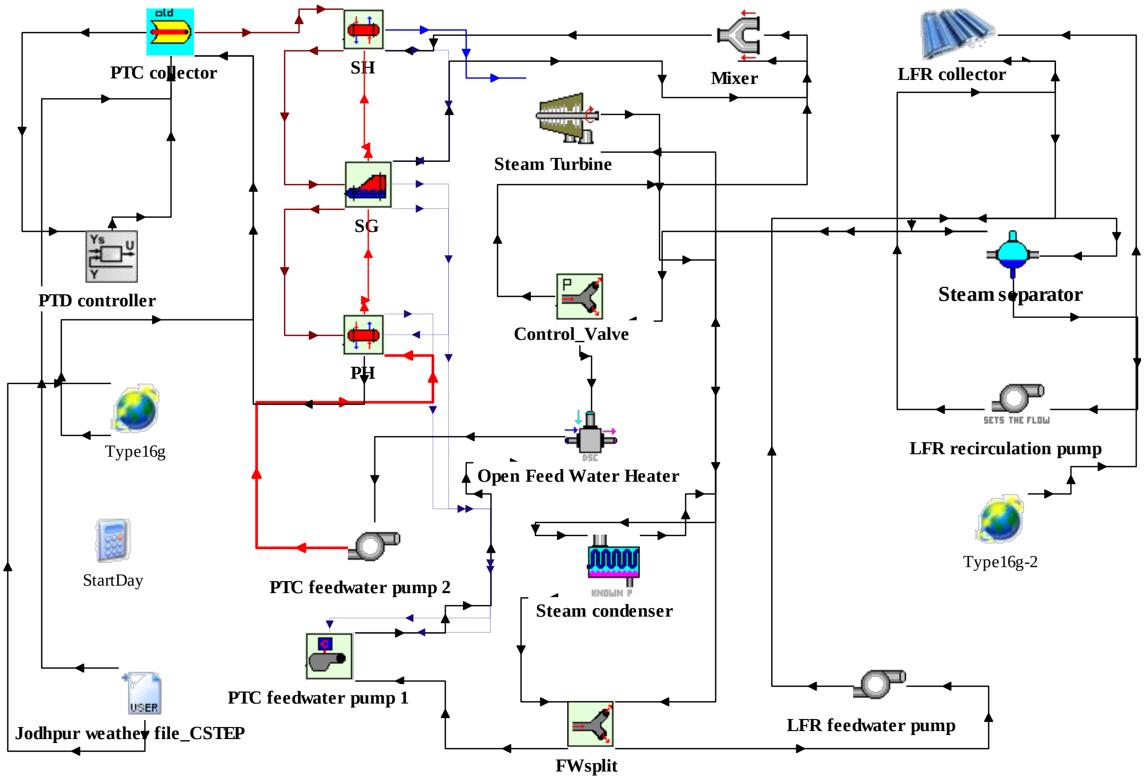

Fig. 4: TRNSYS model of a 1 MWe multi-field STPP with OFWH

Fig. 4 shows a TRNSYS model of a 1 MWe multi-field STPP with OFWH. A PID controller has been used to control the outlet temperature through tracking fraction by defocusing the PTC collector area. A control valve has been used to direct a controlled source steam mass flow rate to the OFWH from the incoming saturated steam at the steam drum outlet. The cost functions for the various components have been taken from the literature (Desai and Bandyopadhyay. 2015). The economic modelling was predicated on a 10% discount rate and a thirty-year plant life. The annual simulation of a techno-economic model results in the STPP producing net amounts of electricity. The annual electricity production was utilized in calculating the plant's LCOE.

$$\mathrm{LCOE} = \frac{(C_{\mathrm{equipment}} + C_{\mathrm{misc}} \cdot \dot{W}_{\mathrm{gen,kWe}} + C_{\mathrm{civil}} + C_{\mathrm{land}}) \cdot \mathrm{CRF} + (C_{\mathrm{O\&M}})}{E_{\mathrm{gen}}} \qquad \text{(eq. 3)}$$

where E_{gen}= Net annual electric energy generation (kWh)

$\dot{W}_{\mathrm{gen,kWe}}$= Net electric power capacity or name-plate capacity (kWe)

C_{civil} and C_{land} = Civil work and land cost ($)

$C_{\mathrm{equipment}}$ = Equipment cost of the power block and solar field system components ($)

C_{misc}= miscellaneous cost ($ kWe^{-1})

$C_{\mathrm{O\&M}}$= operation and maintenance cost ($)

CRF = capital recovery factor = $\frac{d \cdot (1+d)^n}{(1+d)^n - 1}$; *d* = discount rate and *n* = plant life

4. Results and discussion

Fig. 5 depicts the monthly net electric energy generated by a 1 MWe multi-field STPP with and without an OFWH configuration and the related effective direct normal irradiation (EDNI). The total amount of energy entering a surface per unit area under direct normal irradiation is known as EDNI. It should be noted that the electric energy yield is significantly higher with OFWH than without it for nearly every month of the year. It also demonstrates that the generation of electric energy depends on the EDNI of the location. In October, the Jodhpur location recorded its highest EDNI of 198.1 kWh m-2 month-1, resulting in a net electric generation of 0.24 GWh. Conversely, July marked the lowest electric energy generation, with an EDNI of 93.2 kWh m-2 month-1, responsible for a net electric generation of 0.07 GWh. This results from the monsoon's seasonal influence on the region, constituting a cloud cover.

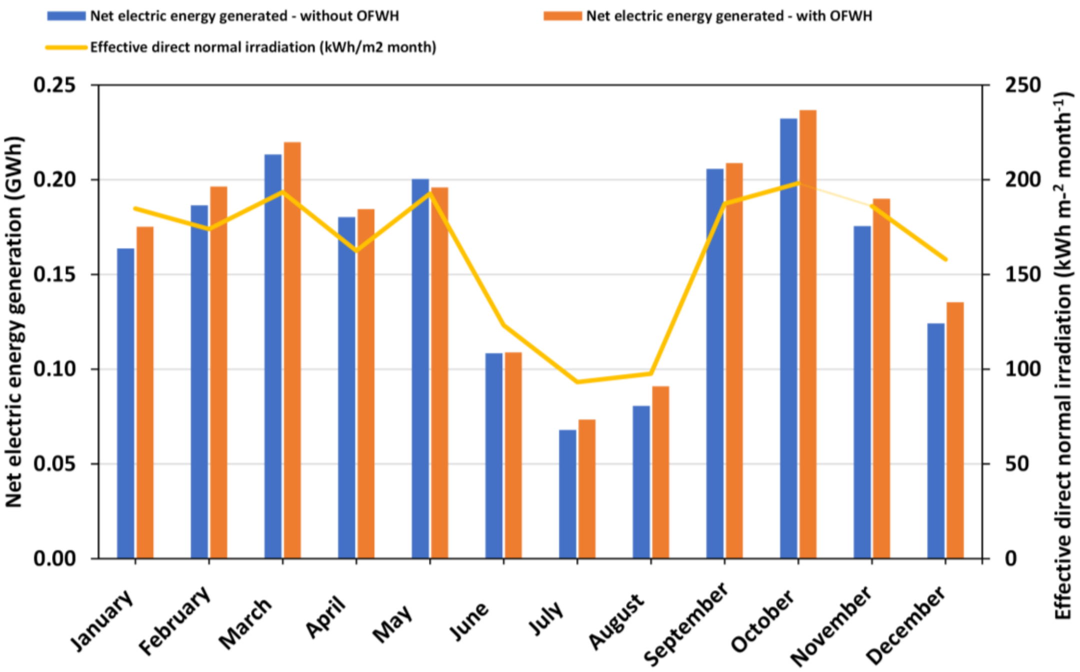

Fig. 5: Monthly net electric energy generation comparison of a 1 MWe multi-field STPP without and with OFWH and the corresponding effective direct normal irradiation

The monthly variations in the LFR collector efficiency of the OFWH and the multi-field configuration performance efficiency are depicted in Fig. 6. It can be seen that LFR collector efficiency for both configurations remains almost the same, irrespective of their design thermal capacity. Nonetheless, the OFWH operated with a nearly constant thermal efficiency from October to April, when the LFR useful heat generation remained high. However, from May to July, the OFWH's thermal performance declined due to insufficient useful heat generation of the LFR solar field; this also impacted the power plant's net electric energy generation, as depicted in Fig. 5. The impact of AR on the STPP's performance and LCOE is highlighted in Table 4. Higher AR tends to reduce the design thermal capacity of the preheater and PTC solar field, reducing the capital cost of the STPP. Furthermore, the design thermal capabilities of the preheater and OFWH are practically the same.

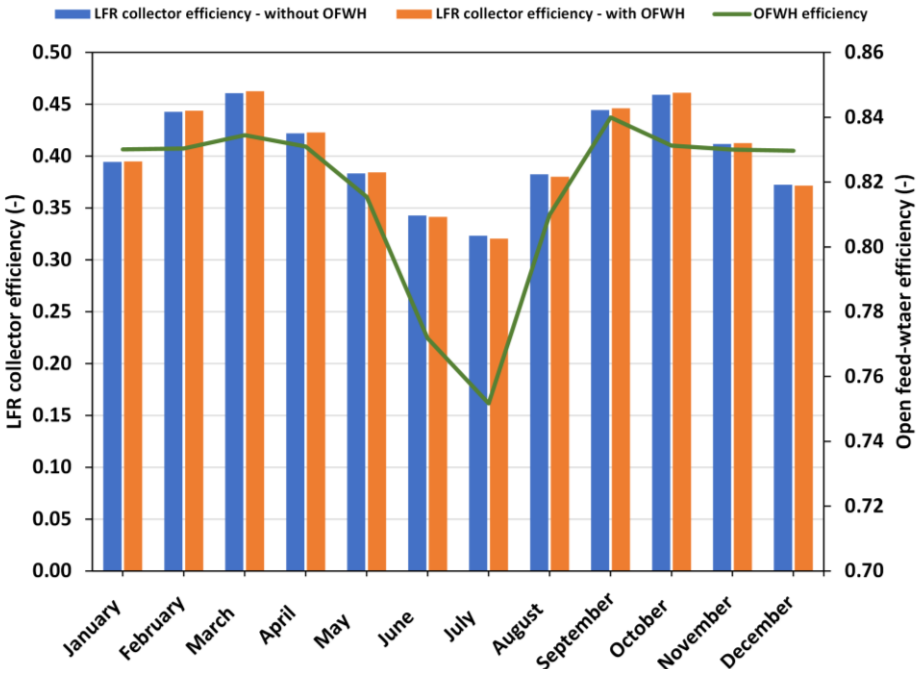

Fig. 6: Monthly variation of LFR collector efficiency of a 1MWe STPP multi-field configuration with and without OFWH and Open feed water heater efficiency

As a result, the OFWH uses less energy for preheating. However, the net electric energy generation is slightly higher at low AR. This is due to the increased gross capacity of the turbine power. All these factors tend to improve the economics of power generation, reducing the LCOE.

Table 4: Performance and LCOE variation at two different aperture area ratios (AR) of a 1 MWe multi-field STPP

Aperture area ratio (AR)	Annual heat energy extracted from OFWH	Annual heat energy transfer from preheater	Annual useful heat energy collected from LFR solar field	Net annual electric energy generated	LCOE
(-)	(GWh)	(GWh)	(GWh)	(GWh)	($/kWh)
1.15	0.57	1.16	5.85	2.12	0.332
4.14	0.21	0.24	8.69	2.02	0.306

In Table 5, the outcomes of a techno-economic analysis are presented, along with a comparison to the configuration that does not incorporate the open feedwater heater for the proposed multi-field configuration. It compares the LCOE obtained for the proposed configuration to the LCOE obtained for a multi-field configuration without an OFWH using the TRNSYS model, the literature model, and a simulation from (Desai and Bandyopadhyay, 2015).

Table 5: Techno-economic comparison of a multi-field STPP with and without open feedwater heater integration

Description	Area of LFR	Area of PTC	Net annual electric energy generated	LCOE
	(m^2)	(m^2)	(GWh)	(\$ kWh^{-1})
Literature (without open feedwater heater) (Desai and Bandyopadhyay, 2015)	9500	3500	-	0.326
Our model (without an open feedwater heater)	9500	3500	1.94	0.324
Our model (with an open feedwater heater)	10832	2617	2.02	0.306

It was found that the LCOE of the suggested multi-field setup with a feedwater heater is 5.5% lower than the LCOE of the configuration without the open feedwater heater. This is due to lower upfront costs for the PTC collecting area and heat exchanger units and an increased low-cost LFR solar field area.

5. Conclusion

A novel 1 MWe multi-field STPP configuration with open feed water integrated at the LFR steam drum output has been proposed to improve the LCOE of electric energy generation in Jodhpur, India. A techno-economic study was performed for a given configuration, and the LCOE was compared with a multi-field STPP configuration without an open-feed water heater. An aperture area ratio was used in a design parametric study, which revealed that the STPP constructed with larger aperture area ratios helps lower the STPP's capital cost and, thus, the LCOE. Compared to a configuration lacking an open-feed water heater, the novel configuration results in a 5% reduction in the LCOE.

References

Desai, N. B., and Bandyopadhyay, S., 2015. Integration of parabolic trough and linear Fresnel collectors for optimum design of concentrating solar thermal power plant. Clean Technologies and Environmental Policy, 17(7), 1945–1961.

Giostri, A., Binotti, M., Astolfi, M., Silva, P., Macchi, E., Manzolini, G., 2012. Comparison of different solar plants based on parabolic trough technology. Solar Energy. 86(5), 1208–1221.

Giostri, A., Binotti, M., Silva, P., MacChi, E., Manzolini, G., 2013. Comparison of two linear collectors in solar thermal plants: Parabolic trough versus Fresnel. Journal of Solar Energy Engineering, Transactions of the ASME. 135(1), 1–9.

Gunther, M., 2011. Advanced CSP Teaching Materials - Linear Fresnel Technology. Advanced CSP teaching materials.

Islam, M. T., Huda, N., Abdullah, A. B., & Saidur, R., 2018. A comprehensive review of state-of-the-art concentrating solar power (CSP) technologies: Current status and research trends. Renewable and Sustainable Energy Reviews. 91, 987–1018.

Klein, S. A., Duffie, J. A., Mitchell, J. C., Kummer, J. P., Thornton, J. W., Bradley, D. E., Arias, D. A., Beckman, W. A., Duffie, N. A., Braun, J. E., Urban, R. E., Blair, N. J., McDowell, T. P., Duffy, M. J., 2018. TRNSYS 18: A Transient System Simulation Program. Getting Started (Vol. 1).

Manzolini, G., Giostri, A., Saccilotto, C., Silva, P., Macchi, E., 2011. Development of an innovative code for the design of thermodynamic solar power plants part B: Performance assessment of commercial and innovative technologies. Renewable Energy. 36(9), 2465–2473.

Morin, G., Dersch, J., Platzer, W., Eck, M., Häberle, A., 2012. Comparison of Linear Fresnel and Parabolic Trough Collector power plants. *Solar Energy*, *86*(1), 1–12. https://doi.org/10.1016/j.solener.2011.06.020

Nayak, J. K., Kedare, S. B., Banerjee, R., Bandyopadhyay, S., Desai, N. B., Paul, S., Kapila, A., 2015. A 1 MW national solar thermal research cum demonstration facility at Gwalpahari, Haryana, India. In Current Science (Vol. 109, Issue 8, pp. 1445–1457). https://doi.org/10.18520/v109/i8/1445-1457

Ramaswamy, M. A., Suresh, N. S., Rao, B. S., Thirumalai, N. C., 2013. Estimation of Hourly Direct Normal Irradiance(DNI). Center for Study of Science, Technology and Policy (CSTEP).

Schenk, H., Hirsch, T., Feldhoff, J. F., Wittmann, M., 2014. Energetic comparison of linear Fresnel and parabolic trough collector systems. Journal of Solar Energy Engineering, Transactions of the ASME. 136(4), 1–11.

Schwarzbözl, P., Eiden, U., Pitz-Paal, R., & Jones, S., 2002. A TRNSYS Model Library for Solar Thermal Electric Components (STEC). A Reference Manual Release 2.2.

Shang, Z., 2000. Analysis and optimization of total site utility systems, Doctor of Philosophy. Department of Process Integration University. University of Manchester Institute of Science and Technology,UK, (Issue August).

Thornton, J. W., Bradley, D. E., McDowell, T. P., Blair, N. J., Duffy, M. J., LaHam, N. D., Naik, A. V., 2012. TESSLibs 17 - Combined Heat and Power (CHP) / Cogeneration Library Mathematical Reference (Vol. 13).

TRANSSOLAR Energietechnik GmbH., 2017. TRNSYS 18 (Vol. 3).